БЪЛГАРСКА АКАДЕМИЯ НА НАУКИТЕ
ТЕОРЕТИЧНА И ПРИЛОЖНА МЕХАНИКА
София, 1983, год. XIV, № 1

BULGARIAN ACADEMY OF SCIENCES
THEORETICAL AND APPLIED MECHANICS
Sofia, 1983, Year XIV, No. 1

On the Instability of a Liquid Capillary Jet Flowing into an Immiscible Liquid

St. Radev, B. Chavdarov, Iv. Penchev

1. Introduction

The problem about the capillary instability of a liquid jet flowing into a medium of immiscible liquid finds practical application in a numbers of apparatus in chemical industry, such as extractors, granulators, etc. The capillary instability of a cylindrical jet and its control lie on the basis of non-inertial jet printing devices, employed in modern computers.

A series of papers have been dedicated to the instability of a liquid capillary jet in a linear treatment [1-8]. In [1] the instability of an nonviscous liquid jet flowing into vacuum has been discussed. The jet viscosity is accounted for in equations for a perturbed flow in [2,3], assuming uniform velocity profiles of the basic stream. An analogous problem but with taking into account viscosity of the surrounding liquid has been solved in [4-8]. The solutions cited so far are mainly qualitative since the substitution of the real velocity profiles by uniform ones is quite a crude approximation. In [9] the real velocity profiles are considered and the perturbed flow equation is solved numerically by shooting method.

To compare the numerical and experimental results the length of the non-broken jet section is employed which is easy to determine experimentally with satisfactory accuracy. A detailed experimental study for determining the effect of the physico-chemical properties of fluids on the jet length has been made in [10,11]. An approximation method is proposed in [12] to calculate the length of a cylindrical jet, while [13-15] offer a method for calculating jet length accounting for its contraction.

The present paper offers a numerical solution of the equation of perturbed flow by the method of differential Gauss elimination (see[17]). The radius and the velocity profile of the basic stream are obtained from the numerical solution of Prandtl equations by the method offered in [16]. An experimental study was carried out in this work to establish the influence of the geometric form of the nozzle upon the jet length. A comparison was made between the numerical and the experimental results on the jet length.

2. Setting of the problem

The flow of an axisymmetric jet of a viscous liquid, interacting with a viscous surrounding medium is described by the equations of Navier-Stokes. At the jet surface the conditions for continuity of velocity and tangential

stresses as well as the condition of discontinuity of the normal stresses and the condition of nonpenetrability are satisfied. At the jet axis are satisfied the conditions of symmetry while at infinity — transformation of the flow into a uniform unperturbed stream. Our aim is to investigate the instability of a steady flow just by using the method of small perturbations.

We initiate a cylindrical coordinate system Ozr in such a way that the z-axis is directed along the length of the jet and the origin of the coordinate system is placed at the center of the nozzle. As characteristic scales we choose the radius of the nozzle R_N and the maximum outflow velocity U_N.

We introduce a stream function Ψ_j for the velocity field of the perturbed flow $\{U_j, V_j\}$ in the following manner:

$$U_j = \frac{1}{r}\frac{\partial}{\partial r}(r\Psi_j), \quad V_j = -\frac{\partial \Psi_j}{\partial z} \quad (j=1, 2)$$

Here and further on the index 1 designates the parameters and functions of the jet flow, whereas the index 2 designates those of the surrounding medium.

We are searching for a partial solution of the stream function in the form of a running wave along the z axis:

$$\Psi_j(z, r, t) = \Phi_j(r)\, exp\,(i\alpha z + \omega t), \quad \omega = \omega_r + i\omega_i$$

wherein α is the wave number related to the perturbation wave length by the expression: $\lambda = 2\pi/\alpha$; ω_r signifies the degree of time growth perturbation.

In a quasiparallel setting, we obtain the Orr-Sommerfeld equation for the amplitude $\Phi_j(r)$ (see[9]):

$$(1) \qquad (U_j - c)(L - \alpha^2)\Phi_j + \left(\frac{U_j'}{r} - U_j''\right)\Phi_j = \frac{\nu_j}{\nu_1 i\alpha Re}(L - \alpha^2)\Phi_j \quad (j=1, 2)$$

$$L \equiv \frac{d}{dr^2} + \frac{1}{r}\frac{d}{dr} - \frac{1}{r^2}$$

denoting $c = i\omega/\alpha$; $Re = U_N R_N/\nu_1$ is the Reynolds number; ν_j are the kinematic viscosities; U_j are the velocity profiles of the steady flow.

The conditions of symmetry at the jet axis and the condition at infinity give respectively:

$$(2) \qquad \Phi_1 = \Phi_1'' = 0, \quad r = 0$$

$$(3) \qquad \Phi_2 \to 0, \ \Phi_2' \to 0, \quad r \to \infty.$$

From the continuity of the velocity field and tangential stresses at the jet surface and from discontinuity of the normal stresses there, follow the corresponding boundary conditions:

$$[\Phi] = 0, \left[\Phi' - \frac{\Phi U'}{U - c}\right] = 0, \quad r = h(z)$$

$$\left[\mu\left(L\Phi + \alpha^2\Phi - \frac{U''\Phi}{U - c}\right)\right] = 0,$$

$$(4) \qquad \left[\frac{\mu}{\mu_1 i\alpha Re}\left\{(L\Phi)' + \frac{1}{r}L\Phi - \alpha^2\left(3\Phi' + \frac{\Phi}{r}\right)\right\}\right] -$$

$$-\left[\frac{\rho}{\rho_1}\left\{(U - c)\left(\Phi' + \frac{\Phi}{r}\right) - U'\Phi\right\}\right] = -\frac{(1 - \alpha^2 r^2)\Phi_1}{We\, r^2 (U_1 - c)},$$

wherein the square brackets denote the value of discontinuity along the outer normal at the interface; μ_j and ρ_j are respectively dynamic viscosity and density; $We=\rho_1 U_N^2 R_N/\sigma$ is Weber's number.

When the wave number α is given, the problem (1)—(4) is an eigenvalue problem for the complex parameter c, whereby the searched eigenvalue c is enclosed non-linearly in the boundary condition (4). The iteration method is employed in the present work to find one eigenvalue and the differential Gauss elimination method is applied to each iteration. For the velocity profiles of the steady flow U_j and for the unperturbed jet radius $h(z)$ we use the numerical results obtained by the method proposed in [16].

3. Outline of the numerical method

By the following set up:

$$v_1=\Phi_1,\quad v_2=(L-\alpha^2)v_1,\quad v_3=v_1'+\frac{1}{r}v_1,\quad v_4=v_2'+\frac{1}{r}v_2$$

$$w_1=\Phi_2,\quad w_2=(L-\alpha^2)w_1,\quad w_3=w_1'+\frac{1}{r}w_1,\quad w_4=w_2'+\frac{1}{r}w_2$$

we obtain from the Orr-Sommerfeld equation two systems of linear first-order equations:

(5) $$\mathbf{v}'=M_1\mathbf{v},\quad \mathbf{v}=(v_1, v_2, v_3, v_4)^T$$

$$M_1=\begin{bmatrix} -\frac{1}{r} & 0 & 1 & 0 \\ 0 & -\frac{1}{r} & 0 & 1 \\ \alpha^2 & 1 & 0 & 0 \\ m_1 & m_2 & 0 & 0 \end{bmatrix}$$

$$m_1=i\alpha Re\left(\frac{U'}{r}-U''\right)$$

$$m_2=\alpha^2+i\alpha Re(U-c)$$

(6) $$\mathbf{w}'=M_2\mathbf{w},\quad \mathbf{w}=(w_1, w_3, w_2, w_4)^T$$

$$M_2=\begin{bmatrix} -\frac{1}{r} & 1 & 0 & 0 \\ \alpha^2 & 0 & 1 & 0 \\ 0 & 0 & -\frac{1}{r} & 1 \\ m_3 & 0 & m_4 & 0 \end{bmatrix}$$

$$m_3=i\alpha Re\,\frac{\nu_1}{\nu_2}\left(\frac{U'}{r}-U''\right)$$

$$m_4=\alpha^2+i\alpha Re\,\frac{\nu_1}{\nu_2}(U-c)$$

The boundary conditions (4) we write down in the terms of the new variables as scalar products:

(7) $$(\mathbf{l}_{1,k}, \mathbf{v})+(\mathbf{l}_{2,k}, \mathbf{w})=0\quad (k=1, 2, 3, 4)$$

Condition (2) is transformed into:

(8) $$v_1=v_2=0,\quad r=0$$

At infinity $U_2\to U_\infty=\text{const}$ and the Orr-Sommerfeld equation has an analytical solution:

$$w_1 = C_1 K_1(\alpha r) + C_2 K_1(\beta r)$$

wherein K_1 is a modified Bessel function and $\beta^2 = \alpha^2 + i\alpha \frac{\nu_1}{\nu_2} Re(U_\infty - c)$. For $w_2 = (L - \alpha^2) w_1$ we obtain $w_2 = C_2(\beta^2 - \alpha^2) K_1(\beta r)$.

Using the asymptotic form $K_1(r) \sim \frac{C_1 e^{-r}}{\sqrt{r}}$ at a distance far enough from the jet surface we obtain the relationship:

$$(9)\quad (w_2, w_4)^T = B^*(w_1, w_3)^T,\ r = r^*,\ B^* = \begin{bmatrix} (\alpha+\beta)\left(\frac{1}{2r^*} - \alpha\right), & -(\alpha+\beta) \\ (\alpha+\beta)\left(\frac{1}{2r^*} - \alpha\right)\left(\frac{1}{2r^*} - \beta\right), & -(\alpha+\beta)\left(\frac{1}{2r^*} - \beta\right) \end{bmatrix}$$

On this manner we transform the problem (1)—(3) into the following:

$$(10)\quad \mathbf{v}' = M_1 \mathbf{v},\quad M_1 = \left[\begin{array}{c|c} K_1 & G_1 \\ \hline D_1 & E_1 \end{array}\right],\quad r \in (0, h)$$

$$(11)\quad v_1 = v_2 = 0,\quad r = 0$$

$$(12)\quad \mathbf{w}' = M_2 \mathbf{w},\quad M_2 = \left[\begin{array}{c|c} K_2 & G_2 \\ \hline D_2 & E_2 \end{array}\right],\quad r \in (h, r^*)$$

$$(13)\quad (w_2\ w_4)^T = B^*(w_1, w_3)^T,\quad r = r^*$$

wherein $K_j, G_j, D_j, E_j\ (j = 1, 2)$ are 2×2 matrices.

We are, looking for the subspace of the solutions of (10) which satisfy condition (11) i. e. we are looking for the relationship:

$$(14)\quad (v_1, v_2)^T = A(r)(v_3, v_4)^T,\ A(r) = \begin{bmatrix} a_{11}(r) & a_{12}(r) \\ a_{21}(r) & a_{22}(r) \end{bmatrix},$$

wherein the functions a_{ij} at any point $r \in (0, h)$ define one and the same subspace of solutions which satisfy (11). For the function a_{ij}, using (10), we obtain the Cauchy problem, written in a matrix form:

$$(15)\quad A' = G_1 + K_1 A - A E_1 - A D_1 A,\quad r \in (0, h)$$

$$(16)\quad A(0) = 0$$

For the matrix $B(r) = \begin{bmatrix} b_{11}(r) & b_{12}(r) \\ b_{21}(r) & b_{22}(r) \end{bmatrix}$, which satisfies the relationship

$$(w_2, w_4)^T = B(w_1, w_3)^T$$

we have analogically:

$$(17)\quad B' = D_2 + E_2 B - B K_2 - B G_2 B,\quad r \in (h, r^*)$$

$$(18)\quad B(r^*) = B^*$$

The solutions of systems (15)—(16) and (17)—(18) at the point $r = h(z)$ we designate A^h and B^h respectively. If we write down the boundary conditions (7) in a matrix form:

$$(19)\quad H \cdot \mathbf{s} = 0,\quad \mathbf{s} = (v_3, v_4, w_1, w_3)^T,\quad H = H_{4\times 4}(c\,; A^h, B^h)$$

the determinant of H must vanish to provide a non-trivial solution of the initial problem (1)—(4). This condition gives the required eigenvalue relation. In

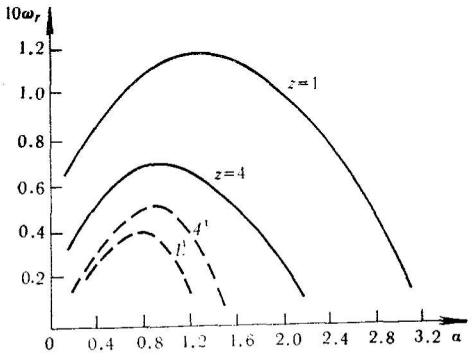

F ig. 1 Dependence of the perturbation growth c oefficient ω_r on the wave number α
$\rho_0=\rho_2/\rho_1=1000$, $\mu_0=\mu_2/\mu_1=50$, Re=100, We=100, Fr=10

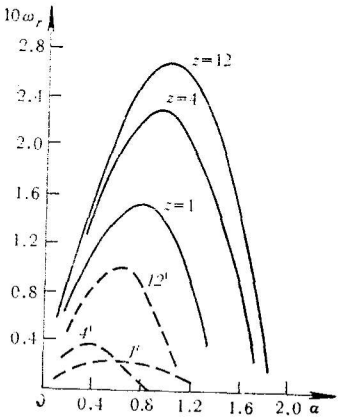

Fig. 2 Dependence of the perturbation growth coefficient ω_r on the wave number α
$\rho_0=1.6$, $\mu_0=0.969$, Re=653.87, We=5.51, Fr=16

actual calculations, of course, some iterative procedure must be performed until this condition is satisfied to some prescribed degree of accuracy.

In the program implementation, systems (15)—(16) and (17)—(18) are integrated by the Runge-Kutta method [18]. To find the searched eigenvalue c we iterate by the method of parabolae which is not so sensitive to initial approximations.

The eigenvalues are computed with relative error of $10^{-4} \div 10^{-5}$.

One of the advantages of the method of differential Gauss elimination lies in that we do not integrate the Orr-Sommerfeld equation directly, which in the case of large Reynolds numbers is troublesome. On the other hand the solutions of systems (15)—(16) and (17)—(18) are monotonous functions (as distinct from those of (1)) which allows a large step of integration. Unlike the shooting method [9] it is not necessary here to use asymptotics of the solution in the vicinity of $r=0$, whereas integration is performed directly from $r=0$.

4. Numerical results

Fig. 1 shows the dependency of the perturbation growth coefficient ω_r on the wave number α for a water jet, flowing out into air. The solid lines correspond to a parabolic initial velocity profile, whereas the dotted lines correspond to flat profiles in the same cross sections. Curves 1 and 1′ refer to section $z=1$ while curves 4 and 4′ — to section $z=4$. The results obtained lie close to the results in [9]. A comparison between the curves in the above figure indicates a strong influence of the velocity profile upon ω_r. When only contraction of the jet is accounted for (flat profiles—curves 1′ and 4′) the instability area is widened up along the jet, whereas, if both the development of a velocity profile and jet contraction are taken into consideration (curves 1 and 4) this area is narrowed down. The latter effect is due to the fact that the velocity profile gradient rapidly decreases along the z-axis (in this case we have a weak interaction with the surrounding medium) and despite the jet contraction the jet becomes more stable.

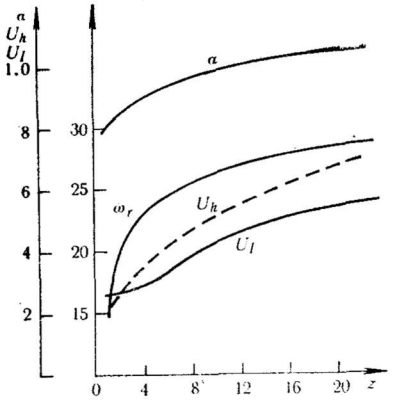

Fig. 3 Alteration of the maximum perturbation growth coefficient ω_r, its corresponding wave number α, phase velocity of the fastest growth perturbation U_l and surface velocity U_h along the jet
μ_0=0.969, Re=653.87, We=5.51, Fr=16

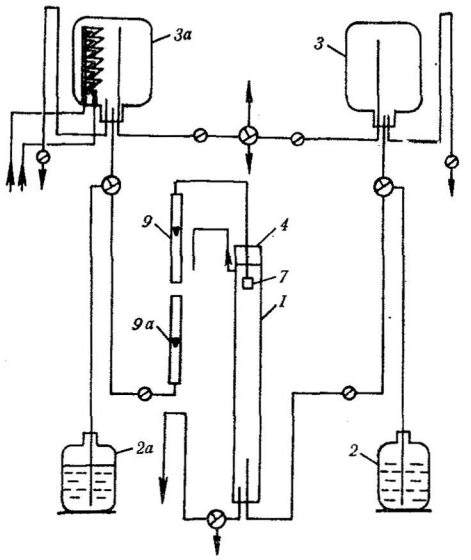

Fig. 4 Scheme of the experimental set-up

Fig. 2 illustrates the same dependence $\omega_r=\omega_r(\alpha)$ but in a case of a carbon tetrachloride jet, with a parabolic initial profile, flowing out into a standing water medium. The dotted curves are obtained with the same velocity profiles and radii of the jet as those of the solid curves but without accounting for the interaction with the surrounding medium (in the problem of instability). The destabilizing influence of the interaction with the medium is clearly seen on a comparison between curves 1, 4, 12 and 1′, 4′, 12′ respectively. In contrast to Fig. 1, the instability area and maximum growth coefficient here increase with the development of the jet which is due to the weaker decrease of velocity profile gradient as a result of the strong interaction between the jet and medium.

Fig. 3 refering to the same case, described in Fig. 2, shows the alteration of maximum growth coefficient ω_r, its corresponding wave number α, the basic velocity at the jet surface U_h and the phase velocity of the fastest growth perturbation $U_l=-\frac{\omega_i}{\alpha}=c_r$, as the jet flows down. It is evident from the figure that the wave length of the fastest growth perturbation decreases along the jet. It is characteristic for all four curves that they are practically saturated at $z>20$.

5. Description of the experimental set up and experimental results

The magnitudes characterizing jet instability, for which experimental methods of determination have been developed, are the wave length of perturbance and the length of unbroken jet section. Determination of the wave length

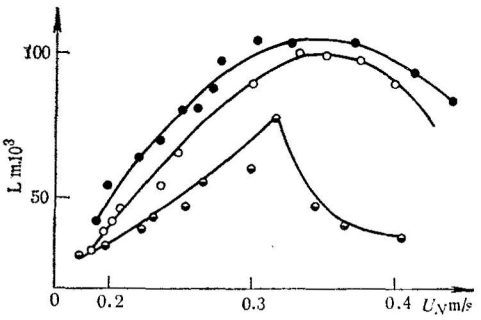

Fig. 5 Dependence of the length of unbroken jet on the mean outflow velocity for a brass nozzle in case of carbon tetrachloride jet in water

ρ_0=1.6, μ_0=0.969, σ=46.5.10^{-3} N/m

●$\frac{L}{D_N}$=115, ○ $\frac{L}{D_N}$=50, ⊙$\frac{L}{D_N}$=10

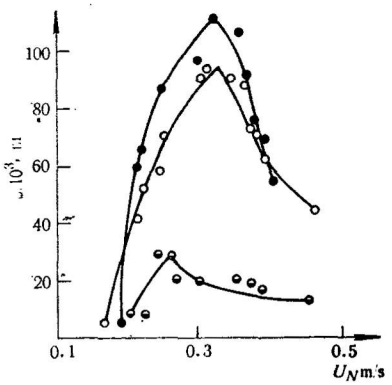

Fig. 6 Dependence of the length of unbroken jet on the mean outflow velocity for a glass nozzle in case of carbon tetrachloride jet in water

●$\frac{L}{D_N}$=51, ○$\frac{L}{D_N}$=31, ⊙=11

of perturbance is difficult and associated with a high error. For this reason the jet length is employed for the experimental check of the numerical results.

A scheme of the experimental set-up is shown in Fig. 4. It represents a glass column 1 with a diameter of 0.08 m and height of 1.2 m, at the top of which the dispersed phase is fed in. The nozzles are connected with the tube for feeding in the dispersed phase through a teflon ring. In this manner a quick easy change of nozzles can be made. Flow-rate of the dispersed phase, flowing from the tank vessel 3^a is checked by means of rotameters 9 and 9^a. The length of the unbroken jet section is measured from a photograph. Each experimental point is obtained as an average value of data from five photographs.

Fig. 5 and Fig. 6 illustrate the results on the alteration of the jet length as a function of the mean outflow velocity for three brass and three glass nozzles with a diameter of 2.10^{-3}m and different lengths of the inlet nozzle section, indicated in each figure. These figures allow a judgment about the influence of the inlet section length of the nozzle upon the jet instability. Jets flowing out of a nozzle with a short inlet section are significantly more unstable than those flowing out of a longer one. This is due to both the form of the initial jet profile and the fact that the not-yet-shaped profile is a "carrier" of much higher perturbations.

The value of the initial perturbation is a quantity which is convenient for a qualitative evaluation of the influence of the inlet nozzle section upon the jet instability. It is determined by minimizing the functional:

$$\delta = \sum_{i=1}^{n} \left[Z_i - \frac{U_{N,i}}{\omega_{r,i}} ln\left(\frac{1}{h_0}\right) \right]^2 \qquad (20$$

wherein:

Z_i is the measured jet length under the condition of the i^{th} test

$U_{N,i}$ is the mean outflow velocity from the nozzle during i^{th} test

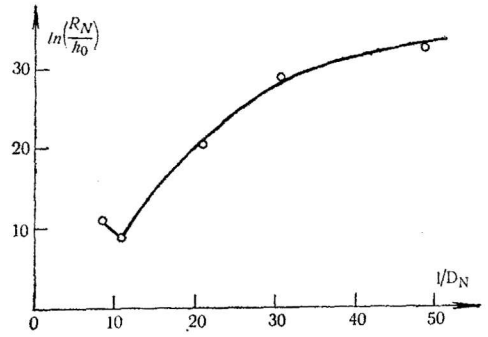

fig. 7 Dependence of the value of initial perturbation on the length of inlet nozzle section for a brass nozzle in case of carbon tetrachloride jet in water

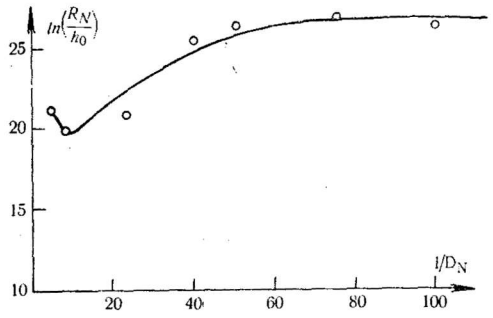

Fig. 8 Dependence of the value of initial perturbation on the length of inlet nozzle section for a glass nozzle in case of tetrachloride jet in water

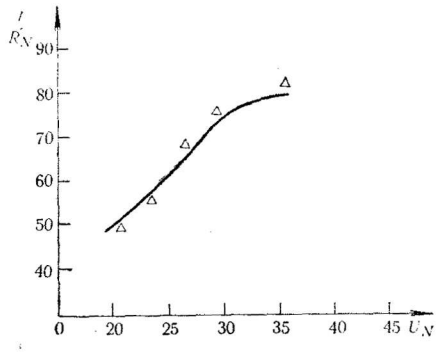

Fig. 9 A comparison between the numerical and the experimental results on the jet length for a glass nozzle $l_N/D_N=5$ in case of carbon tetrachloride jet in water
$\rho=1.6$, $\mu=0.969$, Δ—experiment

ω_{ri} is the degree of perturbation growth under the conditions of the i^{th} test, calculated by the dispersion equation offered in (5)

$\bar{h}_0$ — amplitude of the initial perturbation

n — the total number of tests for a given nozzle

Fig. 7 and Fig. 8 show the alteration of magnitude of the initial perturbation $ln\left(\frac{1}{\bar{h}_0}\right)$ in dependence of the inlet section length of the nozzle for glass and brass nozzles respectively. Obviously, the jet is most stable with a well shaped laminar profile at the nozzle outlet which corresponds to the longest nozzle. At the same time, the other extreme case which corresponds to a flat velocity profile formed at a "zero" length of the inlet section, also leads to a decrease of initial perturbation. The material of which the nozzle is made affects the jet instability to a much lesser extent.

In Fig. 9 the experimental and numerical results are compared for the jet length of carbon tetrachloride flowing out into water. The nozzle is one glass with a length-diameter ratio of 5. Numerically the jet length is calculated by

the method proposed in [13—15] aproximating the perturbation amplitude $\bar{h}$ at a finite number of cross sections recurrently by the formula:

$$\bar{h}_k=\bar{h}_{k-1}\,exp\left[\omega_{r,\,k-1}\frac{z_k-z_{k-1}}{U_{I,\,k-1}}\right] \tag{21}$$

herein $\bar{h}_k=\bar{h}(z_k)$, $U_{I,\,k}=U_I(z_k)$; $\omega_{r,\,k}=\omega_r(z_k)$ is the maximum perturbation growth cofficient at z_k section.

We calculate while $\bar{h}_k>h(z_k)$. Then z_k is taken as a jet length. The initial perturbation amplitude is chosen as $ln\ (1/\bar{h}_0)=22.3$. The figure shows that in the discussed range of outflow velocities, the numerical and the experimental results are in a satisfactory agreement.

6. Conclusion

The numerical and experimental studies carried out indicate that jet instability is influenced by two factors which have oppositely directed effects on it. On the one hand, as the jet develops, it contracts under the influence of surface tension and gravitational forces, which act destabilizing on the jet. On the other hand, as the jet develops, there is a tendency of velocity profile flattening which is more markedly expressed when the interaction with the surrounding medium is weak. The ratio between these two oppositely directed effects determines the degree of jet instability in each given case.

The experiments carried out show that the type and the inlet nozzle section length affect jet instability via initial velocity profile and the magnitude of initial perturbation.

A comparison between the experimental and numerical results on the jet length shows that the presented theory describes satisfactoryly the jet instability in the case of moderate outflow velocities.

Received 5.10.1982

References

1. Релей (Дж. Стрэтт), Теория звука, ОГИЗ, Москва, 1944.
2. Weber, C., ZAMM, **11**, 136 (1931).
3. Левич, В. Г., Физико-химическая гидродинамика, Физматгиз, М., 1959.
4. Tomotika, S., Proc. Roy. Soc., **A150**, 322 (1935).
5. Assenov, A. A., I. P. Penchev, S. P. Radev, Theor. Appl. Mech. **8**, 35 (1977).
6. Meister, B. J., Ph. D. Thesis, Cornell Univ., Itaka, New York (1966).
7. Дитякин, Ю. Ф., Л. А. Клячко, Б. В. Новиков, В. А. Ягодкин, Распыливание жидкостей, М., Машиностроение, 1977.
8. Лышевский, А. С., Изв. ВУЗ — Энергетика, № 7 97, 1960.
9. Епихин, В. Е., В. Я. Шкадов, Изв. АН СССР, МЖГ, № 6, 50 (1978).
10. Meister, B. J., G. F. Scheele, AIChE Journal, **15**, 689 (1969).
11. Takahashi, T., Y. Kitamura, Kagaku Kogaku, **35**, 637 (1970).
12. Smith, S., H. Moss, Proc. Roy. Soc., **A93**, 373 (1917).
13. Ziabicki, A., R. Takserman-Krozer, Roczniki Chemii, **37**, 1607 (1963).
14. Takahashi, T., Y. Kitamura, Kagaku Kogaku, **35**, 1229 (1970).
15. Penchev, I., S. Radev, Theor. Appl. Mech. (bulg.), **8**, 16 (1977).
16. Gospodinov, P., I. Penchev, S. Radev, Int. J. Mult. Flow. **5**, 87 (1979).
17. Гольдштик, М. А., В. Н. Штерн, Гидродинамическая устойчивость и турбулентность, Н. Новосибирск, 1977.
18. Форсайд, Д., М. Мальком, К. Моуер, Машинные методы математических вычислений, М., 1980.